Pitching Characteristics of Peripheral Jet Ground Effect Machines

By

Hiroshi MAEDA*

(Received March 31, 1967)

A theory of the pitching characteristics is presented for three-dimensional peripheral jet ground effect machines which are equipped with a compartment partition along the pitch axis. The analysis is separated into two parts, i.e. the longitudinal static stability and the dynamic pitching motion. In both cases, the behaviors of jet are quantitatively treated as the underfed and overfed operation.

At the static pitch condition, the cushion pressures in the falling downward and rising upward compartments are first discussed, and applying those results, a simple expression of the static moment about the pitch axis is derived. Next, utilizing the quasi-static principle, a second order nonlinear differential equation is obtained as the equation of pitching motion.

Detailed calculations have been carried out for a circular model GEM, and the comparisons with experimental data are encouraging.

1. Introduction

The static longitudinal stability and the dynamic pitching motion of three-dimensional peripheral jet ground effect machines are so important in practice that these phenomena have recently been studied by several investigators[1-4]. However, since simple and convenient expressions of those phenomena have not been obtained yet, a simplified analysis of the pitching characteristics of three-dimensional GEMs with arbitrary planform is discussed in this report. Fortunately, a simple analysis of the heaving motion of GEMs has already been performed by the author and comparisons with experimental data are encouraging. Therefore, similar concepts are applied in the present analysis, too.

As is well known, original peripheral jet GEMs are unstable or only slightly stable in pitch and roll displacement, and therefore it is necessary in practice to be equipped with stability jets or compartment partitions in order to ensure the adequate stability. The present work deals with GEMs equipped with a compartment partition only.

* Department of Aeronautical Engineering.

Simple assumptions on which the present theory is based are as follows:

(1) The hover height above the ground is constant despite the variation of pitching angle.

2) The forward velocity is zero.

3) Since a compartment partition is attached at the bottom of GEM along the pitch axis, the pressure difference between those compartments is kept constant when the GEM is tilted.

4) The simple momentum theory is applied in the analysis.

5) The jet momentum along the periphery is constant despite the pitching angle.

6) The incompressibility condition is satisfied throughout the motion.

7) The complicating viscious effect of jets is neglected.

The present analysis is separated into two parts, i.e. a theory of pitch stability or a theoretical method of obtaining the restoring moment of a tilting peripheral jet GEM is first discussed, and assuming the quasi-static condition the equation of pitching motion is next derived. The theory is applicable for a peripheral jet GEM with arbitrary planform, but the detailed calculations have been carried out for a circular GEM and compared with experimental data.

2. Theory of Static Stability in Pitch

2.1 Static pitch condition

Let us consider a three-dimensional peripheral jet GEM with arbitrary planform represented in Fig. 1. In this figure, it is assumed that x-axis is the axis of symmetry and in the direction of fore-and-aft, and y-axis is the pitch axis. In the xy plane, the shape of peripheral jet nozzle is expressed by

$$y = f(x) \qquad (1)$$

and a compartment partition to ensure the pitch stability is attached along the y-axis as shown in Fig. 1.

When the GEM is tilted by the

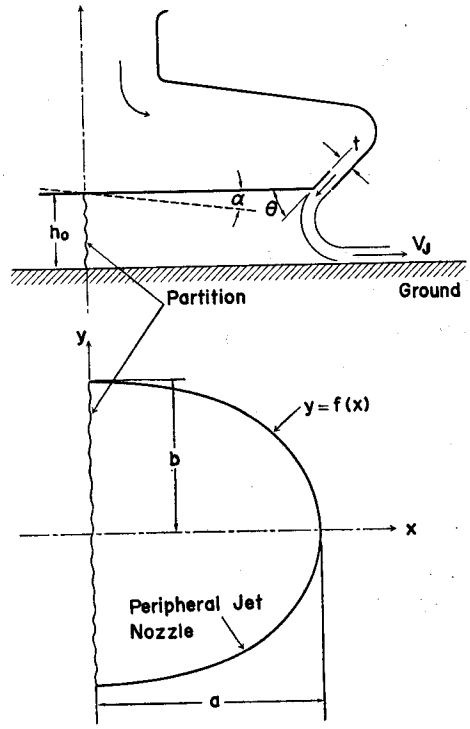

Fig. 1. Configuration of a peripheral jet GEM.

angle of pitch α, the front compartment falls downward and the rear compartment rises upward, and the cushion pressures vary in each compartment. The reason why the cushion pressures vary depends on the following phenomena, i.e.

1) The hover height variation is produced along the bottom surface of GEM.

2) The inclination angle of peripheral jet relative to the horizontal varies along the jet nozzle.

For instance, let us consider an arbitrary point P on the peripheral jet nozzle of the downward compartment as shown in Fig. 2. The hover height variation due to the angle of pitch α is expressed by

$$\Delta h = x \cdot \alpha \qquad (2)$$

In addition, the variation of jet inclination angle becomes

$$\Delta\theta = \alpha \cdot \sin\lambda = \alpha \cdot \frac{y'}{\sqrt{1+y'^2}} \qquad (3)$$

because the jet direction at P is supposed to be normal to the tangent at this point.

At the static pitch condition, it is assumed that the cushion pressures p_d and p_u are constant in each compartment respectively. For instance, in the downward compartment, since the jet momentum is constant along the periphery, the jet momentum

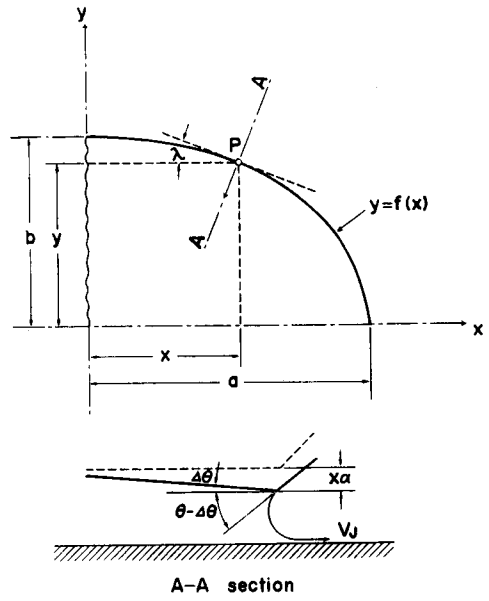

Fig. 2. Peripheral jet nozzle of the downward compartment.

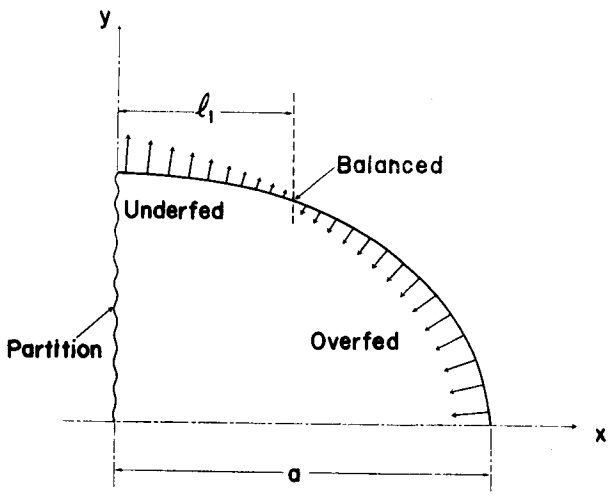

Fig. 3. Flow condition at the downward compartment.

change at the nose part of jet nozzle is too large to the cushion pressure p_d and then overfed conditions are satisfied. On the contrary, the jet momentum change at the region close to the compartment partition is too small to p_d and then underfed conditions are satisfied and consequently the pressurized air will escape to the atmosphere. (see Fig. 3 and Fig. 4) Therefore, the balanced jet condition for p_d will naturally be satisfied at $x=l_1$ which is a point between the overfed and underfed regions.

In the upward compartment, similar conditions will be realized, too.

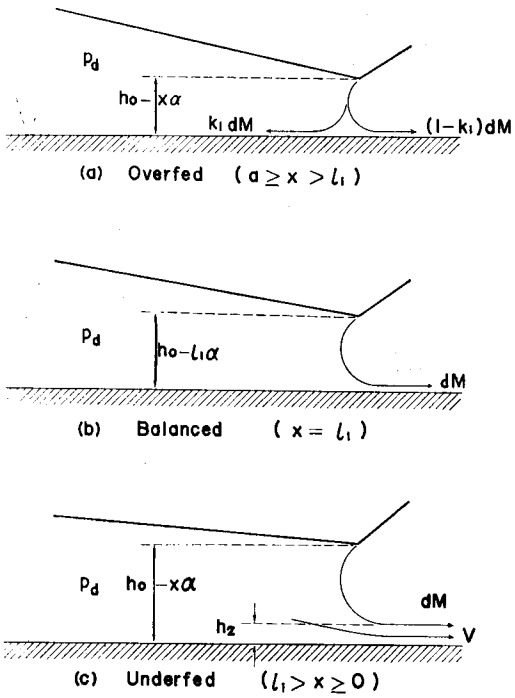

Fig. 4. Overfed, balanced and underfed jet.

2.2 Cushion pressure in the downward compartment

Let us consider the equilibrium conditions of forces in the downward compartment sealed by the jet sheet and the partition. Applying the simple momentum theory, the equations become, using Eq. (2) and (3),

$$p_d(h_0-x\alpha) = dM\cdot\cos\left(\theta-\frac{\alpha y'}{\sqrt{1+y'^2}}\right)+(1-k_1)dM-k_1dM \quad : a\geq x>l_1 \quad (4)$$

$$p_d(h_0-l_1\alpha) = dM\left[1+\cos\left(\theta-\frac{\alpha y'}{\sqrt{1+y'^2}}\right)\right] \quad : x=l_1 \quad (5)$$

$$p_d(h_0-x\alpha-h_2) = dM\left[1+\cos\left(\theta-\frac{\alpha y'}{\sqrt{1+y'^2}}\right)\right] \quad : l_1>x\geq 0 \quad (6)$$

where dM is the peripheral jet momentum per unit length and is given by

$$dM = t\cdot\rho\cdot V_J^2 \quad (7)$$

and h_2 in Eq. (6) is the thickness of air flow which escapes from the underfed region.

Furthermore, the equation of continuity of mass flow becomes

$$\int_0^{l_1}\rho h_2 v\sqrt{1+y'^2}\cdot dx = \int_{l_1}^{a}k_1 t\rho V_J\sqrt{1+y'^2}\cdot dx \quad (8)$$

where v is the escaping velocity of pressurized air and is given by applying Bernoulli's equation,

$$v = \sqrt{\frac{2p_d}{\rho}} \tag{9}$$

Since the function k_1 is considered maximum at $x=a$ and zero at $x=l_1$, then by assuming the linear variation, it becomes approximately

$$k_1 = \frac{k_m}{a-l_1}(x-l_1) \tag{10}$$

where k_m is the maximum value of k_1 at $x=a$.

For simplifying the calculation, since α is in general much smaller than θ and $|y'/\sqrt{1+y'^2}| \leq 1$, then α terms in the r.h.s. of Eq. (4), (5) and (6) can be neglected and the following approximate equations are obtained in place of the above stated equations, i.e.

$$p_d(h_0-x\alpha) = (1+\cos\theta)dM-2k_1dM \quad : a \geq x > l_1 \tag{11}$$

$$p_d(h_0-l_1\alpha) = (1+\cos\theta)dM \quad : x = l_1 \tag{12}$$

$$p_d(h_0-x\alpha-h_2) = (1+\cos\theta)dM \quad : l_1 > x \geq 0 \tag{13}$$

Furthermore, if the cushion pressure at the balanced hover condition, p_b, is introduced,

$$p_b \cdot h_0 = (1+\cos\theta)dM \tag{14}$$

In order to determine the cushion pressure p_d as a function of p_b and α, using Eq. (12) and (13),

$$h_2 = (l_1-x)\alpha \tag{15}$$

Substituting Eq. (9), (10) and (15) into Eq. (8), it is solved in k_m to give

$$k_m = \frac{\sqrt{2p_d \cdot \rho}}{t\rho V_J} \cdot \alpha(a-l_1) \frac{\int_0^{l_1}(l_1-x)\sqrt{1+y'^2}\cdot dx}{\int_{l_1}^{a}(x-l_1)\sqrt{1+y'^2}\cdot dx} \tag{16}$$

Since k_1 is determined by substituting Eq. (16) into Eq. (10), p_d is, after some calculation using Eq. (7), (11) and (12), expressed by

$$p_d = 8\rho V_J^2 \cdot F^2 \tag{17}$$

where

$$F = \frac{\int_0^{l_1}(l_1-x)\sqrt{1+y'^2}\cdot dx}{\int_{l_1}^{a}(x-l_1)\sqrt{1+y'^2}\cdot dx} \tag{18}$$

Eq. (17) is rearranged using Eq. (7), (12) and (14), and the following equation is obtained,

$$\frac{1}{1-\frac{l_1\alpha}{h_0}}\cdot\frac{t(1+\cos\theta)}{8h_0}=F^2 \tag{19}$$

From Eq. (19), l_1 is determined and p_d is given by the following equation

$$p_d=p_b\cdot\frac{1}{1-\frac{l_1\alpha}{h_0}} \tag{20}$$

Eq. (20) is derived from Eq. (12) and (14).

In order to determine the value of l_1 by Eq. (19), it is necessary to assume the configuration of peripheral jet nozzle and calculate the function F. As an example, let us consider a circular GEM with the radius of a. In this case, since the relation between x and y is given by

$$x^2+y^2=a^2 \tag{21}$$

and therefore

$$\begin{aligned}\int_0^{l_1}(l_1-x)\sqrt{1+y'^2}\cdot dx &= al_1\sin^{-1}\frac{l_1}{a}+a\sqrt{a^2-l_1^2}-a^2\\ \int_{l_1}^{a}(x-l_1)\sqrt{1+y'^2}\cdot dx &= al_1\sin^{-1}\frac{l_1}{a}+a\sqrt{a^2-l_1^2}-al_1\cdot\frac{\pi}{2}\end{aligned} \tag{22}$$

and the function F in Eq. (18) is given by

$$F=\frac{\frac{l_1}{a}\cdot\sin^{-1}\frac{l_1}{a}+\sqrt{1-\left(\frac{l_1}{a}\right)^2}-1}{\frac{l_1}{a}\cdot\sin^{-1}\frac{l_1}{a}+\sqrt{1-\left(\frac{l_1}{a}\right)^2}-\frac{l_1}{a}\cdot\frac{\pi}{2}} \tag{23}$$

2.3 Cushion pressure in the upward compartment

In a similar way as the case stated above, the analysis can be carried out for the upward compartment, too. In this case, since the overfed condition will be satisfied at the region close to the partition and the underfed condition will be satisfied at the nose part of the present compartment, the equation of determining the balanced jet position l_2, which corresponds to Eq. (19), becomes

$$\frac{1}{1+\frac{l_2\alpha}{h_0}}\cdot\frac{t(1+\cos\theta)}{8h_0}=G^2 \tag{24}$$

where

$$G=\frac{\int_{l_2}^{a}(x-l_2)\sqrt{1+y'^2}\cdot dx}{\int_{0}^{l_2}(l_2-x)\sqrt{1+y'^2}\cdot dx} \tag{25}$$

Therefore, the cushion pressure p_u is given by

$$p_u=p_b\cdot\frac{1}{1+\frac{l_2\alpha}{h_0}} \tag{26}$$

For example, if a circular GEM with radius of a is assumed as well as the preceding case, the function G is expressed by

$$G=\frac{\frac{l_2}{a}\cdot\sin^{-1}\frac{l_2}{a}+\sqrt{1-\left(\frac{l_2}{a}\right)^2}-\frac{l_2}{a}\cdot\frac{\pi}{2}}{\frac{l_2}{a}\cdot\sin^{-1}\frac{l_2}{a}+\sqrt{1-\left(\frac{l_2}{a}\right)^2}-1} \tag{27}$$

2.4 Static pitching moment

Since the cushion pressures p_d and p_u have been obtained, the restoring moment about the pitch axis is easily determined. (see Fig. 5) To begin with, the pitching moment due to p_d is expressed by

$$M_d=p_d\cdot S_d\cdot x_{Gd} \tag{28}$$

where S_d is the effective area and x_{Gd} is the distance between the pitch axis and the center of pressure of the downward compartment.

In the same way, the pitching moment due to p_u becomes

$$M_u=p_u\cdot S_u\cdot x_{Gu} \tag{29}$$

Accordingly, the total pitching moment or the restoring moment against the angle of pitch α is

$$M_t=M_d-M_u \tag{30}$$

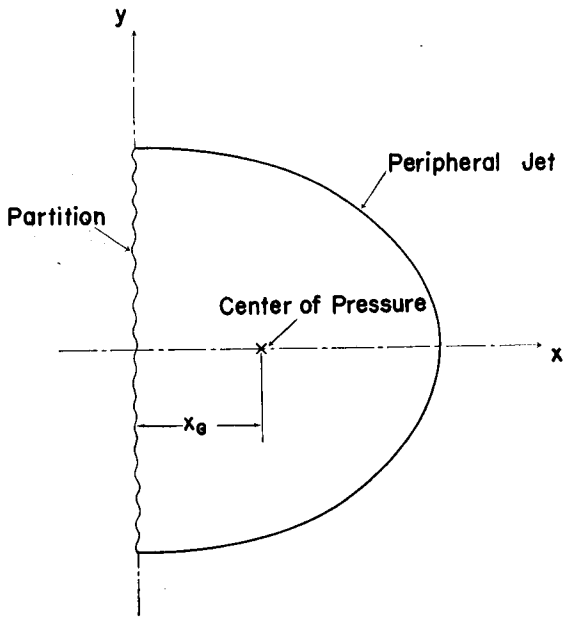

Fig. 5. Restoring moment about the pitch axis.

For example, if a circular GEM with radius of a is assumed,

$$S_d = S_u = \frac{\pi}{2} \cdot a^2$$
$$x_{Gd} = x_{Gu} = \frac{4}{3} \cdot \frac{a}{\pi} = 0.4244a \tag{31}$$

and, accordingly

$$M_t = 0.2122\pi a^3 (p_d - p_u) \tag{32}$$

In order to apply the present result to an arbitrary three-dimensional GEM, it is convenient to represent the restoring moment as another expression. Namely, at the balanced hover condition of a circular GEM,

$$p_b \cdot \pi a^2 = \frac{W}{1 + \dfrac{\sin\theta}{1+\cos\theta} \cdot \dfrac{2h_0}{a}} \tag{33}$$

where W is the total weight of GEM. Substituting Eq. (20), (26) and (33) into Eq. (32),

$$M_t = \frac{0.2122W \cdot a}{1 + \dfrac{\sin\theta}{1+\cos\theta} \cdot \dfrac{2h_0}{a}} \left(\frac{1}{1 - \dfrac{l_1\alpha}{h_0}} - \frac{1}{1 + \dfrac{l_2\alpha}{h_0}} \right) \tag{34}$$

2.5 Numerical examples and comparisons with experimental data

As a numerical example, calculations were carried out for a circular model GEM. The numerical data used are listed below:

$$t = 0.005 \text{ m}, \qquad \theta = 45°, \qquad a = 0.25 \text{ m}$$

Eq. (19) and (24) were first calculated and represented in Fig. 6 and Fig. 7 respectively. As shown in those diagrams, the solution of these equations and accordingly the values of l_1 and l_2 change only slightly for pitching angle variation. Therefore, in this case l_1/a and l_2/a become approximately

$$l_1/a \fallingdotseq 0.42, \qquad l_2/a \fallingdotseq 0.84 \quad : h_0 = 0.030 \text{ m}$$

Consequently, the cushion pressures p_d and p_u are given by

$$p_d = \frac{p_b}{1 - 3.50\alpha}, \qquad p_u = \frac{p_b}{1 + 7.00\alpha} \tag{35}$$

Fig. 8 shows the experimental data and the theoretical results calculated by Eq. (35). The agreement between theory and experiment looks comparatively good in the middle of GEM bottom, but the disagreement is large in proximity to

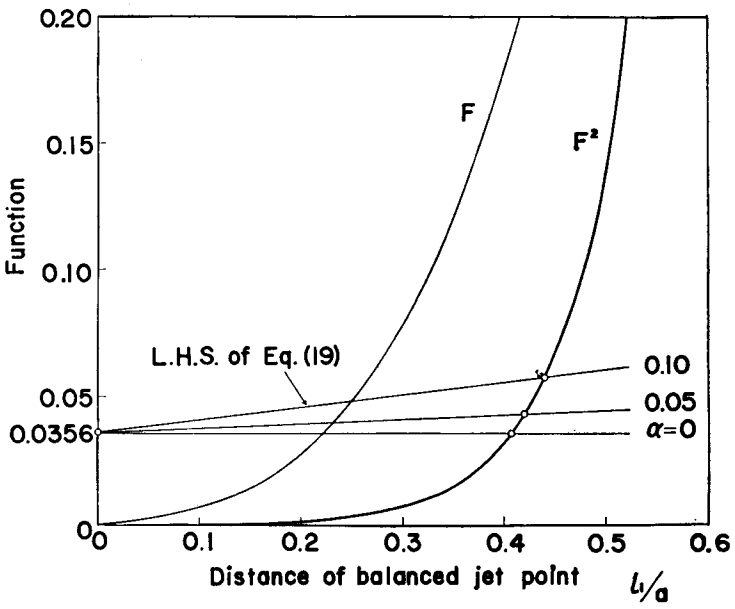

Fig. 6. Determination of the distance of balanced jet point at the downward compartment.

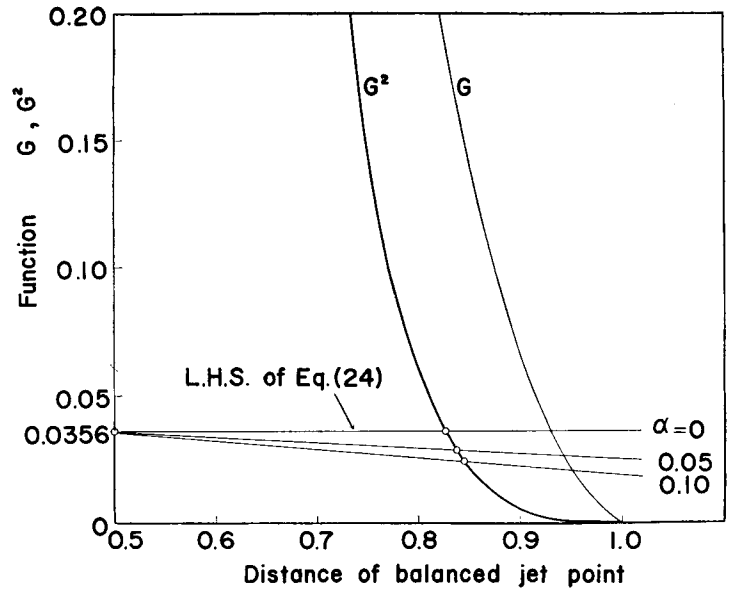

Fig. 7. Determination of the distance of balanced jet point at the upward compartment.

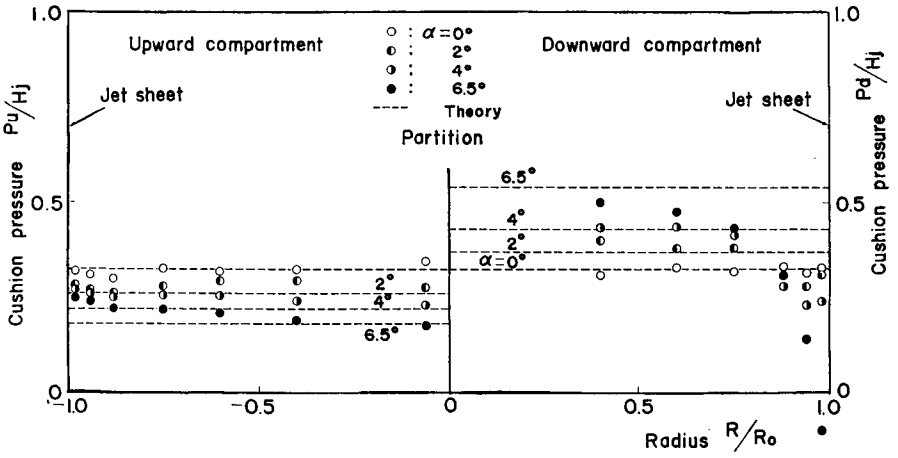

Fig. 8. Cushion pressures of a circlular GEM.

the jet sheet. It is supposed that the reason for this phenomenon depends principally on the entrainment by jet viscous effect.

The static pitching moment was next calculated using the numerical data listed below:

$$W = 2.74 \text{ kg}, \qquad t = 0.005 \text{ m}$$
$$\theta = 45°, \qquad a = 0.25 \text{ m}$$

Since the characteristic lengths l_1 and l_2 are functions of the balanced hover height h_0, they become in this case

$$l_1/a = 0.44, \quad l_2/a = 0.825 \quad : h_0 = 0.0235 \text{ m}$$
$$l_1/a = 0.425, \quad l_2/a = 0.835 \quad : h_0 = 0.0275 \text{ m}$$

and accordingly the cushion pressures p_d and p_u are expressed by

$$\begin{aligned} p_d &= \frac{p_b}{1-4.68\alpha}, \quad p_u = \frac{p_b}{1+8.77\alpha} \quad : h_0 = 0.0235 \text{ m} \\ p_d &= \frac{p_b}{1-3.86\alpha}, \quad p_u = \frac{p_b}{1+7.59\alpha} \quad : h_0 = 0.0275 \text{ m} \end{aligned} \tag{36}$$

Therefore, the pitching moment M_t becomes, using Eq. (34),

$$\begin{aligned} M_t &= 0.135\left(\frac{1}{1-4.68\alpha} - \frac{1}{1+8.77\alpha}\right)^{[\text{kg-m}]} \quad : h_0 = 0.0235 \text{ m} \\ M_t &= 0.133\left(\frac{1}{1-3.86\alpha} - \frac{1}{1+7.59\alpha}\right)^{[\text{kg-m}]} \quad : h_0 = 0.0275 \text{ m} \end{aligned} \tag{37}$$

Fig. 9 shows experimental data and the theoretical results calculated by Eq. (37). The experimental results are slightly smaller than the theoretical curves, and it is supposed that the reason still depends on the entrainment phenomena of jet flow.

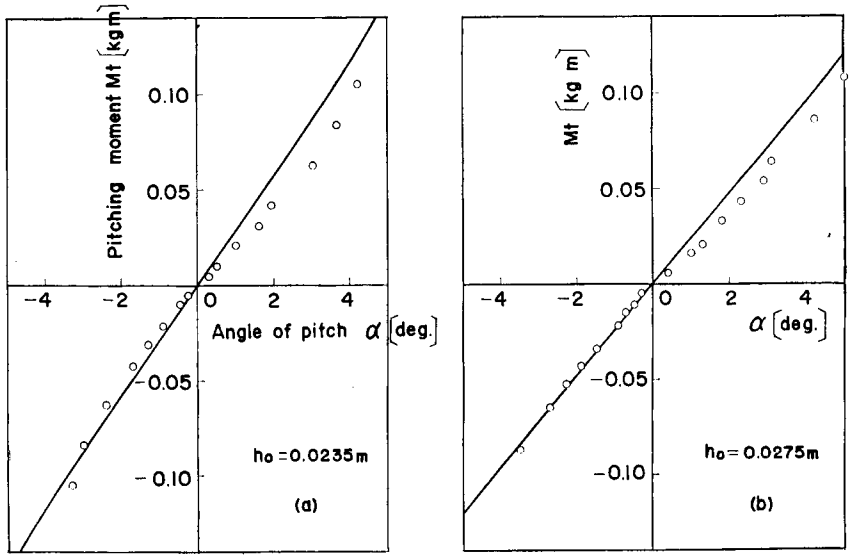

Fig. 9. Static pitching moment.

3. Theory of Dynamic Pitching Motion

Let us consider the dynamic pitching motion of GEM, which means that the pitching angle α is a function of time. If the motion is not so quick, it is satisfactorily assumed that the quasi-static conditions are satisfied, i.e. the results described in the previous sections can still be applied. Therefore, in addition to the preceding analysis, the effect of air volume change due to pitching velocity should be taken into consideration.

3.1 Cushion pressure in the downward compartment

Let us first consider the cushion pressure in the downward compartment during the dynamic pitching motion. (see Fig. 10) In this compartment the cushion air volume decreases in proportion to the pitching velocity $\dot{\alpha}$, and the rate of volume change becomes

$$\dot{V} = 2\dot{\alpha} \int_0^a xy \cdot dx \tag{38}$$

Since this air volume has to escape to the atmosphere with the incompressibility

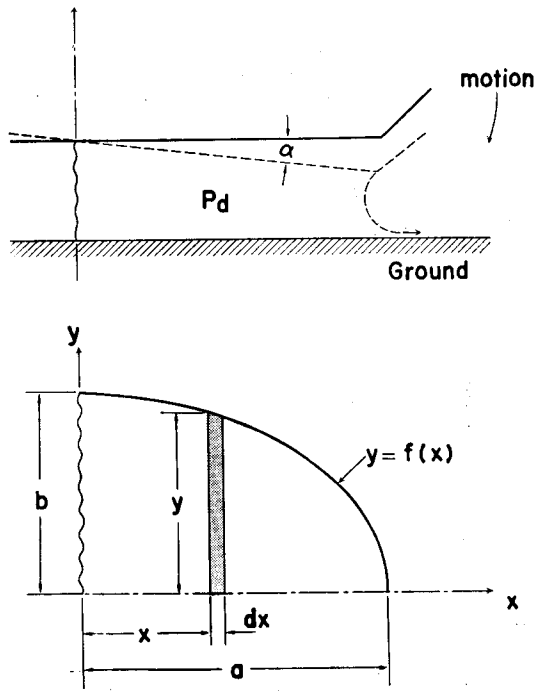

Fig. 10. Rate of air volume change during the dynamic pitching motion.

condition, the following relation should be met, by assuming the uniform flow out of the entire periphery,

$$2\rho h_3 v \int_0^a \sqrt{1+y'^2} \cdot dx = 2\dot{\alpha}\rho \int_0^a xy\, dx \tag{39}$$

where v and h_3 are the escaping flow velocity and thickness respectively. Using the value of v given in Eq. (9),

$$h_3 = \sqrt{\frac{\rho}{2}} \cdot \frac{1}{\sqrt{p_d}} \cdot H \cdot \dot{\alpha} \tag{40}$$

where

$$H = \frac{\int_0^a xy\, dx}{\int_0^a \sqrt{1+y'^2} \cdot dx} \tag{41}$$

On the other hand, using the balanced jet condition at $x=l_1$,

$$p_d(h_0 - l_1\alpha - h_3) = p_b \cdot h_0$$

or

$$\frac{p_b}{p_d} = 1 - \frac{l_1\alpha}{h_0} - \frac{\dot{\alpha}}{h_0} \cdot \sqrt{\frac{\rho}{2}} \cdot \frac{1}{\sqrt{p_d}} \cdot H \tag{42}$$

Solving Eq. (42) in p_d, the cushion pressure is obtained by

$$\frac{1}{\sqrt{p_d}} = \frac{1}{2p_b}\left[-\frac{\dot{\alpha}}{h_0} \cdot \sqrt{\frac{\rho}{2}} \cdot H + \sqrt{\frac{\dot{\alpha}^2}{h_0^2} \cdot \frac{\rho}{2} \cdot H^2 + 4p_b\left(1 - \frac{l_1\alpha}{h_0}\right)}\right] \tag{43}$$

Since $\dot{\alpha}a/V_J \ll 1$ in practice, second order small terms of $\dot{\alpha}a/V_J$ in Eq. (43) can be neglected and the approximate expression of p_d is given by

$$p_d = \frac{p_b}{1 - \frac{l_1\alpha}{h_0}}\left[1 + \frac{1}{\sqrt{2}} \cdot \frac{1}{\sqrt{1+\cos\theta}} \cdot \frac{1}{\sqrt{th_0}} \cdot \frac{1}{\sqrt{1 - \frac{l_1\alpha}{h_0}}} \cdot \frac{\dot{\alpha}}{V_J} \cdot H\right] \tag{44}$$

3.2 Cushion pressure in the upward compartment

In the same way as the preceding case, the cushion air volume increases in proportion to $\dot{\alpha}$ in the upward compartment, and accordingly this air volume has to be supplied with a part of peripheral jet, i.e.

$$2\rho\dot{\alpha}\int_0^a xy \cdot dx = 2 \cdot \Delta t \cdot \rho V_J \int_0^a \sqrt{1+y'^2} \cdot dx \tag{45}$$

or

$$\Delta t = \frac{\dot{\alpha}}{V_J} \cdot H \tag{46}$$

Since the jet momentum decreases in this case, using Eq. (7),

$$dM' = (t - \Delta t)\rho V_J^2 = dM\left(1 - \frac{\Delta t}{t}\right) \tag{47}$$

Furthermore, applying the balanced jet condition at $x = l_2$

$$p_u(h_0 + l_2\alpha) = (1+\cos\theta) \cdot dM' \tag{48}$$

Consequently, the cushion pressure p_u is given by

$$p_u = \frac{p_b}{1 + \frac{l_2\alpha}{h_0}}\left(1 - \frac{1}{t} \cdot \frac{\dot{\alpha}}{V_J} \cdot H\right) \tag{49}$$

3.3 Examples of claculation

The cushion pressures p_d and p_u during the dynamic pitching motion were obtained by Eq. (44) and (49) respectively, but in those equations the function H is undetermined. For example, if a circular GEM with radius of a is assumed, the function H is calculated from Eq. (41) as follows:

$$H = \frac{2}{3\pi} \cdot a^2 \tag{50}$$

Therefore, the cushion pressures p_d and p_u become

$$p_d = p_{d\,\text{static}} \left[1 + \frac{\sqrt{2}}{3\pi} \cdot \frac{1}{\sqrt{1+\cos\theta}} \cdot \frac{a}{\sqrt{th_0}} \cdot \frac{1}{\sqrt{1-\frac{l_1\alpha}{h_0}}} \cdot \frac{\dot{\alpha}a}{V_J} \right] \tag{51}$$

$$p_u = p_{u\,\text{static}} \left[1 - \frac{2}{3\pi} \cdot \frac{a}{t} \cdot \frac{\dot{\alpha}a}{V_J} \right] \tag{52}$$

where $p_{d\,\text{static}}$ and $p_{u\,\text{static}}$ are the values of cushion pressure given in Eq. (20) and (26) in the previous section respectively. Furthermore, in the same way as Eq. (34), the pitching moment M_t during the dynamic pitching motion is expressed by

$$M_t = 0.2122\pi a^3 \cdot p_b \left\{ \frac{1}{1-\frac{l_1\alpha}{h_0}} \left[1 + \frac{\sqrt{2}}{3\pi} \cdot \frac{1}{\sqrt{1+\cos\theta}} \cdot \frac{a}{\sqrt{th_0}} \cdot \frac{1}{\sqrt{1-\frac{l_1\alpha}{h_0}}} \cdot \frac{\dot{\alpha}a}{V_J} \right] \right.$$
$$\left. - \frac{1}{1+\frac{l_2\alpha}{h_0}} \left[1 - \frac{2}{3\pi} \cdot \frac{a}{t} \cdot \frac{\dot{\alpha}a}{V_J} \right] \right\} \tag{53}$$

3.4 Equation of pitching motion

The equation of pitching motion of a GEM is expressed by

$$I\ddot{\alpha} + M_t = 0 \tag{54}$$

where I is the moment of inertia of GEM about the pitch axis.

For example, if a circular GEM with radius of a is assumed, the pitching moment M_t is given by Eq. (53). Therefore, substituting Eq. (53) into Eq. (54), the equation of motion is obtained as follows:

$$I\ddot{\alpha} + M_0 \left[\frac{1}{1-\frac{l_1\alpha}{h_0}} \cdot \frac{\sqrt{2}}{3\pi} \cdot \frac{1}{\sqrt{1+\cos\theta}} \cdot \frac{a}{\sqrt{th_0}} \cdot \frac{1}{\sqrt{1-\frac{l_1\alpha}{h_0}}} + \frac{1}{1+\frac{l_2\alpha}{h_0}} \cdot \frac{2}{3\pi} \cdot \frac{a}{t} \right] \frac{a}{V_J} \dot{\alpha}$$
$$+ M_0 \left[\frac{1}{1-\frac{l_1\alpha}{h_0}} - \frac{1}{1+\frac{l_2\alpha}{h_0}} \right] = 0 \tag{55}$$

where

$$M_0 = \frac{0.2122Wa}{1 + \frac{\sin\theta}{1+\cos\theta} \cdot \frac{2h_0}{a}} \tag{56}$$

Eq. (55) is a nonlinear differential equation, and it can, for instance, be solved by the Isocline method graphically.

As a numerical example, calculations were carried out for a circular model GEM whose numerical data are the same as those used for the calculation of static pitching moment. A theoretical curve calculated is compared with an experiment in Fig. 11.

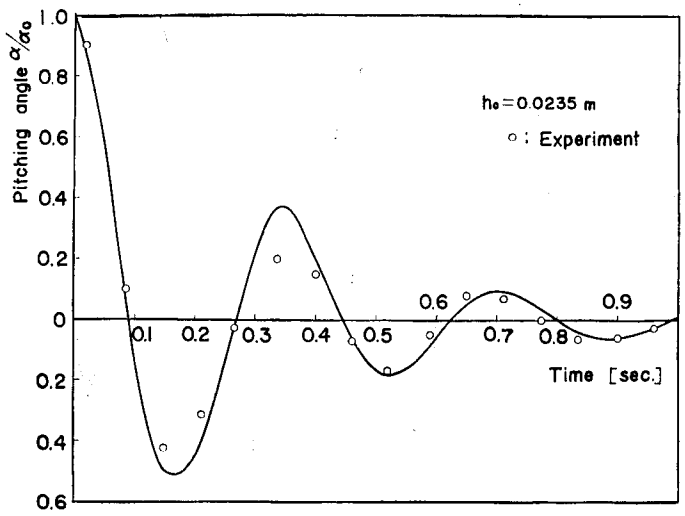

Fig. 11. Time history of pitching oscillation.

In Eq. (55), the third term of this equation is the same expression as the static pitching moment given in Eq. (34). As has been stated in the previous section, the experimental data of static pitching moment are slightly smaller than the theoretical results calculated by Eq. (34). Therefore, in calculating the third term of Eq. (55) numerically, the experimental values in Fig. 9 were used.

Comparisons between the calculated results and experimental data show that the agreement of period of oscillation is comparatively good, but the damping of experimental data looks slightly heavier than that of calculated curve.

4. Concluding Remarks

The pitching phenomena of peripheral jet ground effect machines which are equipped with a compartment partition along the pitch axis were studied and simple expressions of the cushion pressures, static pitching moment and equation of pitching motion were derived.

The analysis is separated into two parts, i.e. the static stability in pitch and the dynamic pitching motion. In the analysis of static stability, the expressions of cushion pressures in the downward and upward compartments were first obtained as functions of the cushion pressure at the balanced hover condition and the angle

of pitch. In addition, using those cushion pressures the static moment about the pitch axis was obtained analytically.

In the derivation of the equation of pitching motion, it was assumed that the quasi-static conditions were satisfied, or in other words the results obtained by the analysis of static pitch stability could be used. A second order nonlinear differential equation was derived as the equation of pitching motion.

As the numerical examples, calculations and experiments were carried out for a circular model GEM. The analytical results were compared with experimental data and the agreement between them found comparatively good.

Notation

a, b : dimensions of peripheral jet nozzle

$$F=\frac{\int_0^{l_1}(l_1-x)\sqrt{1+y'^2}\cdot dx}{\int_{l_1}^{a}(x-l_1)\sqrt{1+y'^2}\cdot dx}$$

$$G=\frac{\int_{l_2}^{a}(x-l_2)\sqrt{1+y'^2}\cdot dx}{\int_0^{l_2}(l_2-x)\sqrt{1+y'^2}\cdot dx}$$

h : hover height

h_0 : hover height at balanced hover condition

h_2, h_3 : escaping flow thickness at underfed condition

$$H=\frac{\int_0^{a}xy\,dx}{\int_0^{a}\sqrt{1+y'^2}\cdot dx}$$

I : moment of inertia of GEM about pitch axis

k_1, k_2 : inflow ratio at overfed condition

l_1, l_2 : x coordinate of balanced jet point

M_t, M_d, M_u : pitching moment

dM : jet momentum per unit nozzle length

p_b, p_d, p_u : cushion pressure

S_d, S_u : cushion area

t : jet thickness

Δt : jet thickness decrement

v : escaping flow velocity of pressurized air

V : cushion air volume

V_J : jet velocity

W : weight of GEM

x, y : Cartesian coordinates
x_{Gd}, x_{Gu} : distance between c.p. and pitch axis
α : angle of pitch
θ : peripheral jet inclination angle
λ : angle between x-axis and tangent at any point on periphery
ρ : air density

dot denotes differentiation with respect to time
prime denotes differentiation with respect to x

References

1) M.C. Eames; IAS Paper, No. 61–71, 1961
2) A.J. Burgess; A.A.S.U. Report, No. 256, 1964
3) G. Kurylowich; UTIAS Report, No. 110, 1965
4) D.I.G. Jones and M. Blake; J. Aircraft, **3**, No. 2, 1966
5) H. Maeda and Y. Kondo; THIS MEMOIRS, **29**, Part 2, 1967